

Evidence of late Holocene climate variability in the western Nanling Mountains, South China

Wei Zhong · Jibin Xue · Jun Ouyang ·
Jiayuan Cao · Zhanghong Peng

Received: 6 March 2013 / Accepted: 19 March 2014 / Published online: 3 April 2014
© Springer Science+Business Media Dordrecht 2014

Abstract A 95-cm-thick peat sequence obtained from Daping Swamp in the western Nanling Mountains provides evidence for climate variability in the past ~3,000 year. Multi-proxy records (including organic carbon isotopes, humification degree, organic matter content, and dry bulk density) revealed three intensified Asian summer monsoon (ASM) intervals (i.e. ~2900–2700, 2500–1700 and 1000–600 cal. yr BP) and three weakened ASM intervals (i.e. ~2800–2500, 1700–1000 and 600–200 cal. yr BP). Our $\delta^{13}\text{C}$ record shows a possible correlation with the sunspot number and residual atmospheric ^{14}C records on multi-centennial scale, especially for the period between 2960 and 2200 cal. yr BP. A spectral analysis of $\delta^{13}\text{C}$ record reveals three significant cycles (i.e., 396, 110 and 102 yr) and all these cycles could be related to solar activity, suggesting that solar output may have influenced the late Holocene climate variability in the study region.

Keywords Late Holocene · Asian monsoon · Solar forcing · Peat · Western Nanling Mountains

W. Zhong (✉) · J. Xue · J. Ouyang · J. Cao
School of Geography Sciences, South China Normal
University, Guangzhou 510631, China
e-mail: DL06@senu.edu.cn

Z. Peng
Department of Social Sciences, Gaozhou Normal School
of Guangdong University of Petrochemical Technology,
Maoming 525000, China

Introduction

Variations in insolation due to orbital changes and solar output over decadal to millennial time scales (Wang et al. 2005) may result in seasonal changes of the land–sea atmospheric pressure distribution and may lead to monsoonal circulation. The Asian monsoon is caused by the thermal difference between the Asian landmass and adjacent oceans that is enhanced by the thermal and dynamic effects of the Tibetan Plateau (An et al. 2001). The Asian Monsoon system, which consists of two important sub-systems, i.e. the east Asian monsoon (EAM) and the Indian monsoon (IM), is an integral part of the global climatic system and plays a significant role in the global hydrological and energy cycles (Cai et al. 2010). The monsoon controls the atmospheric heat budget in the Northern Hemisphere and hence, changes in monsoon have a great potential in controlling global climatic change. Understanding the nature of Asian monsoon variability during the Holocene is essential both to understand the present climatic conditions and to predicting future climatic processes.

Recently, the relationship of paleoclimate changes to the EAM and the IM has attracted the attentions of scholars. Hong et al. (2005, 2010) considered an inverse phase relationship of climate variation between the two monsoons in China. However, Zhang et al. (2011) and Stebich et al. (2011) expressed arguments against such an anti-phase relationship. Thus, these inconclusive results indicate that further

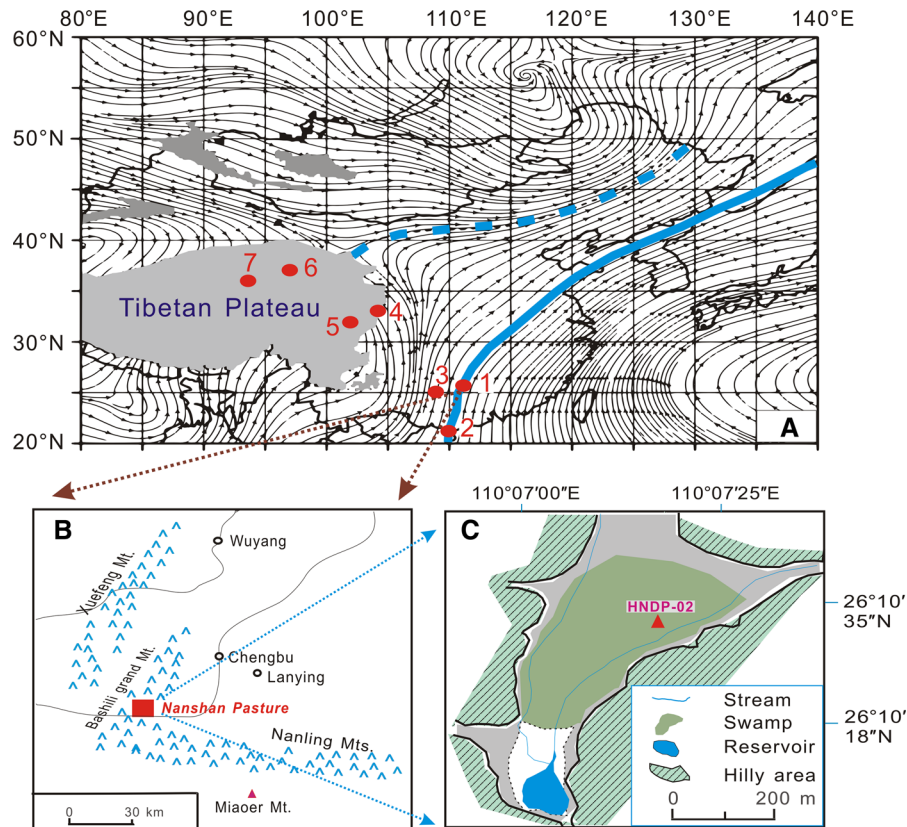


Fig. 1 Climatic background of the subalpine Daping Swamp in the western Nanling Mountains. **a** Decadal means of the moisture (specific humidity) transports in July for 1979–1998 in the lower troposphere (redrawn from Qian et al. (2007); Zhang et al. (2011) with minor modifications). *Dashed blue lines* show the boundaries between westerly and the monsoon moisture. *Solid blue lines* indicate the rough boundaries between Indian summer monsoon and East ASM. Also shown are the locations of various Asian monsoon records in China cited in

Fig. 4: (1) the location of Daping Swamp **b** and the core site **c**, this study); (2) Huguangyan Maar Lake in South China (Yancheva et al. 2007); (3) Dongge Cave in southwest China (Wang et al. 2005); (4) Wanxiang Cave in west Qinling Mountains (Zhang et al. 2008); (5) Hongyuan peat on the eastern fringe of Tibetan Plateau (Hong et al. 2005); (6) Kusai Lake (Liu et al. 2009), and (7) Qinghai Lake (Liu et al. 2006) on the northern and eastern Qinghai-Tibetan Plateau. (Color figure online)

studies are still urgently needed for deciphering the forcing mechanisms responsible for the behaviors of the two monsoon systems.

The Nanling Mountains, which are the watershed between the Yangtze and Zhujiang River systems and act as a very important geographic division of the mid- and south-subtropical zones in China, are located within the area, and they are strongly influenced by the Asian Monsoon (Gao et al. 1962). The western Nanling Mountain (WNLM) region is located in the transitional belt between the EAM and IM systems (Fig. 1a; Qian et al. 2007; Zhang et al. 2011). Detailed paleoclimatic studies of the WNLM will develop the understanding of the

influences of the Asian Monsoon systems on climate change in the monsoonal area of China. In this paper, we present a climatic record derived from a peat section within this region and use these data to explore the history of variations in the Asian monsoon during the late Holocene and investigate possible forcing mechanisms.

Site description

The Daping Swamp is located in the Nanshan Pasture of the Chenbu Miao Nationality Autonomous County in Hunan Province in South China. This region is in the southern Bashili Grand Mountains, part of the

Xuefeng Mountains in the WNLM (Fig. 1b). The present annual average temperature of the region is 10.9 °C, and the average temperatures in January and July are −0.5 and 19 °C respectively. The annual precipitation is about 2,000 mm and the annual evaporation is about 500 mm. Local humidity and temperature conditions mean that the original vegetation was likely dominated by evergreen and deciduous broad-leaved vegetation such as *Machilus rehderi*, *Cyclobalanopsis*, *Fagus* and *Alnus*, as well as shrub vegetation dominated by *Enkianthus*, *Rhododendron* and others (Xiao et al. 1986). However, nowadays, the natural vegetation of this region has been strongly decimated by human activity.

The Daping Swamp is about 300-m long and 150-m wide (Fig. 1c). Geologic investigation has revealed that the accumulation of buried peat accounts for more than 100,000 m³ (Sun and Zhang 1984). Granite bedrock formed a near-surface aquiclude that trapped water and established favorable conditions for peat development in the Daping Basin. A pioneering study on this swamp, performed by Sun and Zhang (1984), indicated that the peaty sediments have promising potential for reflecting past climate change.

Materials and methods

In September 2009, we performed field investigations in this swamp. We selected a 95-cm-thick section (designated section HNBP-02, 26°10.472'N, 110°07.223'E, ~1,620 m a.s.l; Fig. 1c) for our investigation of past climate. Samples were taken at 1-cm intervals for analyses of organic carbon isotopes, humification degree (HD) and loss on ignition. Measurements of dry bulk density (DD) were performed on samples collected at 2-cm intervals.

To exclude the reservoir effect of peat materials, we utilized the method proposed by Zhou et al. (2004). Based on an experiment for peaty sediments, they found that ¹⁴C dating for the bulk portion of the grain size range between 90- and 300-μm fractions can provide reliable dates that agree very well with the pollen accelerator mass spectrometry ¹⁴C ages. Seven bulk samples were collected for conventional radiocarbon dating. We used the Calib 6.0 program and the Intcal 09 data set (Reimer et al. 2009) to calibrate the radiocarbon ages. The chronology of the section was established based on the linear interpolation between neighboring

age levels using the basic (non-Bayesian) age-depth modeling software developed by Blauuw (2010).

To measure organic carbon isotopes (δ¹³C), samples were acid-washed with 5 % HCl to remove traces of carbonate, rinsed with de-ionized water, and oven dried at 50 °C. About 20 mg of each sample were combusted in an excess of oxygen at 1,020 °C by an elemental analyzer. The δ¹³C of the produced CO₂ was measured using a Finnigan MAT-253 Mass Spectrometer. The analytical error is 0.1 ‰. Results are reported in the δ notation relative to the international PDB standard in per mil (‰).

Dry bulk density was measured as the weight of the dry mass per unit volume (Janssens 1983). Dry mass was determined by oven drying at 50 °C until constant weight was achieved. After samples were ground and homogenized, the total organic matter (TOM) was determined by loss on ignition for one and half hours at 550 °C. The fraction below 60 μm was mixed uniformly for measuring the HD. After treatment with 0.1 mol L⁻¹ NaOH and boiling for 1 hour to extract the humic acid, the solution was filtered and diluted. We used a UV-1901 spectrophotometer to measure the absorbance of the solution at a wavelength of 520 nm. The absorbance was expressed relative to the standard value, which was the absorbance of distilled water (defined as 0 %). The absorbance was used to express HD. In this study, we use calibrated HD (HD_{cal}) to indicate the intensity of humification (Zhong et al. 2010b): $HD_{cal} = HD / (M_{sample} \times TOM)$, where HD_{cal} is the corrected absorbance value, HD is the raw absorbance value, M_{sample} is the weight of the sample for measurement, and TOM is the percentage content of TOM represented by loss on ignition. Higher or lower HD_{cal} values represent stronger or weaker humification intensity.

To eliminate the impact of degradation of TOM, the stratigraphic trends of TOM and HD_{cal} were removed using the original data minus their 3-order polynomial fits and the results referred to as TOM_{detrended} and HD_{cal-detrended}.

Results

Lithology and chronology

The lithology of section HNBP-02 is composed primarily of peat (Fig. 2). Below the depth of 95 cm (DP-1), the sediments are dominated by grayish-yellow

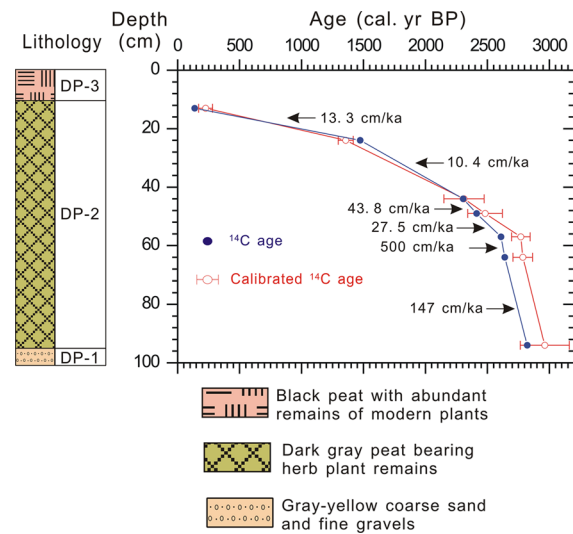


Fig. 2 Lithology and relationship between age and depth of section HNDP-02 in Daping Swamp

coarse sand and fine gravels (≤ 2 cm). The unit from 95–10 cm depth (DP-2) is composed of dark gray peat, mainly bearing herb plant remains. The material of the upper 10 cm in the section (DP-3) consists of black peat with many roots of modern plants and plant remains.

Radiocarbon dating results of the section are listed in Table 1. The bottom age was determined as 2960 cal. yr BP. The average resolution is about 35 years per sample. As illustrated in Fig. 2, the accumulation rates of the upper 50 cm of the section are generally higher than that of the lower part.

Variations of multi-proxy records

In section HNDP-02, the litho-unit DP-1 may originate from the underlying weathered granite crust. The

$\delta^{13}\text{C}$ values range from -30.3 to -28.5 ‰ with a mean value of -29.5 ‰. The HD_{cal} values vary between 21.3 and 69.4 % with an average value of 52.7 %. The DD values range from 0.07 to 0.24 g cm^{-3} with a mean value of 0.12 g cm^{-3} , and the value of TOM fluctuates from 35.5 to 59.7 % with a mean value of 49.4 % (Fig. 3).

Discussion

Climatic implication of $\delta^{13}\text{C}$, HD, TOM and DD

C3 plants exhibit a large range of carbon isotope compositions (-20 – 37 ‰), generally reflecting a physiological response to aridity (anomalously high $\delta^{13}\text{C}$) and a combination of low light levels plus leaf litter recycling (anomalously low $\delta^{13}\text{C}$) (Farquhar et al. 1989). The $\delta^{13}\text{C}$ values of all samples in HNDP-02 section fall within the range of $\delta^{13}\text{C}$ values for C3 plants, suggesting that the peat is dominated by C3 plants. In this study, the influences of both the atmospheric CO_2 and its $\delta^{13}\text{C}$ on the $\delta^{13}\text{C}$ values of C3 plants should be negligible (Feng and Epstein 1995). Investigation of modern C3 plants in north China revealed that a temperature increase of 1 °C causes a decrease in $\delta^{13}\text{C}$ values of C3 plants of ~ 0.3 ‰ (Wang et al. 2002). However, it is unlikely that the amplitudes of variation of $\delta^{13}\text{C}$ values in the section (1.73 ‰) are caused solely by temperature. A number of studies have demonstrated that the $\delta^{13}\text{C}$ values of C3 plants are also sensitive to humidity or precipitation, the higher the humidity or precipitation, the lower the $\delta^{13}\text{C}$ values (White et al. 1994; Hong et al. 2001; Hatté et al. 2001; Chen et al. 2006). A broad compilation of modern carbon isotope

Table 1 Radiocarbon dating results for section HNDP-02 in Daping Swamp in western Nanling Mountains

Lab. code	Field code	Depth (cm)	^{14}C age (a BP)	Calibrated age		Material
				a BP (2σ)	Intercept age	
LUG09-109	DP01-07	10–13	137 ± 44	169–282	230	TOC
LUG09-108	DP01-06	22–25	1474 ± 45	1296–1417	1360	TOC
LUG09-107	DP01-05	42–45	2304 ± 59	2149–2473	2310	TOC
LUG10-120	DP02-03	47–50	2413 ± 69	2342–2621	2480	TOC
LUG09-105	DP01-03	55–58	2610 ± 50	2695–2845	2770	TOC
LUG09-106	DP01-04	62–65	2640 ± 50	2706–2865	2785	TOC
LUG10-119	DP02-02	92–95	2821 ± 82	2765–3161	2960	TOC

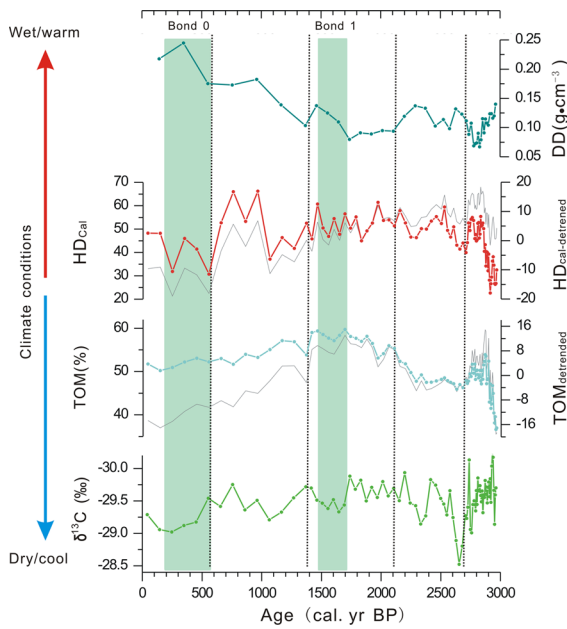


Fig. 3 Variations of multi-proxy records in section HNBP-02 in Daping Swamp. The light gray lines indicate the original data of TOM and humification degree. The blue bars indicate two dry and cold periods that possibly correspond to the North Atlantic ice-rafting events (i.e., Bond events 1 and 0, Bond et al. 2001). (Color figure online)

composition in all C3 plant types also shows a distinct but nonlinear increase in $\delta^{13}\text{C}$ values with decreasing mean annual precipitation (Kohn 2010). In north China, an increase in precipitation by 100 mm corresponds to a decrease in the $\delta^{13}\text{C}$ value of C3 plants by 0.5 ‰ (Wang et al. 2003). Although the exact relationship between the $\delta^{13}\text{C}$ of C3 plants and temperature and precipitation in southern China remains unclear, we infer that values of $\delta^{13}\text{C}$ in section HNBP-02 that are more negative would indicate relatively warmer and wetter conditions, whereas $\delta^{13}\text{C}$ values that are more positive imply a cooler and drier climate.

HD is a proxy to describe the degree of decomposition of plant remains. As the process of decomposition of dead plants is related closely to local climatic conditions, this proxy is a useful indicator of the sedimentary environment and past climatic change (Aaby 1976; Chambers et al. 1997; Christopher and John 2000; Charman et al. 2001; Wang et al. 2010; Zhong et al. 2010). Some experimental studies have revealed a nonlinear influence of water and temperature conditions on the decomposition intensity of

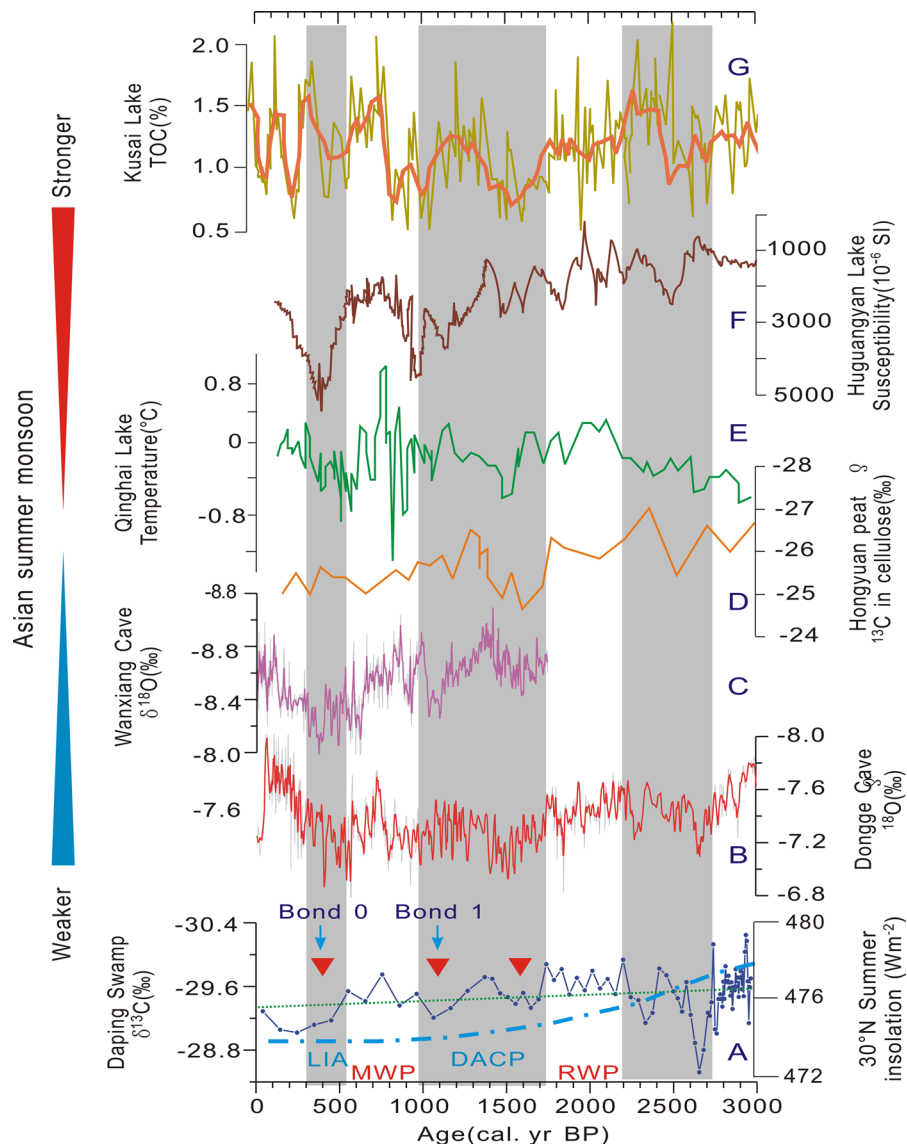
plants (Chai 1990). The ability of microbes to decompose plant remains is weak when the soil temperature is below 5 °C and when the soil humidity is less than 20 %. With increases in both the temperature and humidity of soil, the activity of microbes is rapidly enhanced and peaks when the soil temperature is about 30 °C and when the soil humidity is around 60 to 80 % (Chai 1990). Therefore, conditions that are warmer and more humid promote vegetation production (i.e., higher TOM) and provide more plant remains for decomposition, thus leading to an increase of humic acids in peat. In contrast, dry and cool conditions lead to a reduction in vegetation production (i.e., lower TOM) and weakened microbial decomposition, which results in a decrease in the humic acids in peat. Therefore, higher and lower values of $\text{HD}_{\text{cal-detrended}}$ reflect relatively wet and warm versus dry and cool conditions, respectively.

The DD record can provide information related to climatic conditions regarding the external input of clastic materials into the peat. Increased surface vegetation cover around the swamp in response to the wet and warm conditions would decrease surface erosion, limiting the input of clastic materials and resulting in a reduction of DD values. Conversely, dry and cool conditions would result in lower TOM and higher DD values.

Climate variability in the past ~3,000 years

As shown in Fig. 3, multi-proxy records show poor correlations before 2900 cal. yr BP. From ~2900 to 2700 cal. yr BP, lower $\delta^{13}\text{C}$ and DD values as well as sharp increases in $\text{TOM}_{\text{detrended}}$ and $\text{HD}_{\text{cal-detrended}}$ suggest a wetter and warmer climate, which may have resulted from an intensified summer monsoon. Low $\text{TOM}_{\text{detrended}}$ and relatively higher DD values displayed between 2700 and 2500 cal. yr BP, together with two peak intervals of $\delta^{13}\text{C}$ values, indicate drier and cooler conditions that were probably caused by a weakening of the Asian summer monsoon (ASM) intensity. Lower $\delta^{13}\text{C}$ and DD values as well as higher $\text{TOM}_{\text{detrended}}$ and $\text{HD}_{\text{cal-detrended}}$ between 2500 and 1700 cal. yr BP reflect enhanced precipitation caused by a strengthening in ASM intensity. This interval may correspond to the Roman Warm Period (Desprat et al. 2003). This warm period has also been detected in the Dongge stalagmite record (2300–2100 yr BP) in southwest China (Dykoski et al. 2005), Huguangyan

Fig. 4 Correlation of the $\delta^{13}\text{C}$ record of Daping Swamp with the summer solar insolation at 30°N (Berger and Loutre, 1991), stalagmite $\delta^{18}\text{O}$ records of Dongge Cave (Dykoski et al. 2005) and Wanxiang Cave (Zhang et al. 2008), the magnetic susceptibility of Huguangyan Maar Lake (Yancheva et al. 2007), TOC record of Kusai Lake (Liu et al. 2009), Alkenone-based temperature of Qinghai Lake (Liu et al. 2006), and $\delta^{13}\text{C}$ in cellulose of Hongyuan peat (Hong et al. 2005) RWP, DACP, MWP and LIA represent the Roman warm period, the Dark Age cold period, the medieval warm period, and the Little Ice Age, respectively. The green line indicates the varying trend of Daping $\delta^{13}\text{C}$ record. The red triangles denote three main periods of glacier advances in the southeastern Tibetan Plateau (Yang et al. 2008) The blue arrow lines indicate the intervals that correspond to the Bond Events 1 and 0 (Bond et al. 2001). (Color figure online)



Lake in Leizhou Peninsula of northern tropical China (~ 2500 – 1500 cal. yr BP, Yancheva et al. 2007), Qinghai Lake (~ 2500 – 1600 cal. yr BP, Liu et al. 2006), and Kusai Lake on the Tibetan Plateau (~ 2500 – 1800 cal. yr BP) (Liu et al. 2009; Fig. 4). A decadal resolution temperature reconstruction for the extratropical Northern Hemisphere (90 – 30°N) over the last two millennia indicates warm conditions from 1 AD to 300 AD, during which temperatures may have reached the 1961–1990 AD mean temperature level (Ljungqvist 2010).

Distinct increase in DD (Fig. 3) since 1700 cal. yr BP afterwards and lower accumulation rate in the upper

part of the section (~ 30 cm depth upward, Fig. 2) may result from more input of clastic materials possibly due to the drier and cooler conditions. Gradual increase in $\delta^{13}\text{C}$ decreases in both $\text{TOM}_{\text{detrended}}$ and $\text{HD}_{\text{cal-detrended}}$ suggest a dry and cool period (~ 1700 – 1000 cal. yr BP) that may have been caused by a weakening of the ASM intensity until ~ 1000 cal. yr BP. This period is characterized by two dry and cool periods (1700–1500 and 1300–1000 cal. yr BP) separated by a short wet and warm interval (1500–1300 cal. yr BP). Similar climatic conditions have also been revealed in the stalagmite $\delta^{18}\text{O}$ records in Dongge Cave (~ 1700 – 900 yr BP, Dykoski et al. 2005) and Wanxiang Cave in the western

Qinling Mountains (~200–950 AD, Zhang et al. 2008), the TOC record of Kusai Lake (~1700–1000 cal. yr BP; Liu et al. 2009), the temperature record of Qinghai Lake (~1600–1000 cal. yr BP, Liu et al. 2006), the Ti record of Huguangyan Lake (~1500–900 cal. yr BP; Yancheva et al. 2007), and the cellulose $\delta^{13}\text{C}$ record of Hongyun peat (1800–1300 cal. yr BP, Hong et al. 2005; Fig. 4). This period may correspond to the Dark Age cold period.

A significant increase in $\text{HD}_{\text{cal-detrended}}$ and lower $\delta^{13}\text{C}$ values between 1000 and 500 cal. yr BP indicate wetter and warmer conditions resulting from a strengthened ASM intensity. This agrees well with the results derived from the stalagmite $\delta^{18}\text{O}$ record in Wanxiang Cave (Zhang et al. 2008), and the sediments of Qinghai Lake (~1000–600 cal. yr BP, Liu et al. 2006) and Kusai Lake (~1050–1300 AD, Liu et al. 2009). This warm and wet period correlates well with the medieval warm period. From 500–200 cal. yr BP, higher values of $\delta^{13}\text{C}$, lower values of $\text{HD}_{\text{cal-detrended}}$, a significant increase in DD, and a decrease in $\text{TOM}_{\text{detrended}}$ possibly imply a dry and cool interval, which correlates with the Little Ice Age.

The reconstruction of glacial advance on the southeast Tibetan Plateau also supports our interpretation. Three main periods of glacial advance around 1920–1400 AD, 1150–800 AD, and 600–200 AD (Yang et al. 2008) correspond to the three cool periods identified in section HN2P-02 (i.e., 1700–1500, 1300–1000, and 500–200 cal yr BP). The two cool periods 1700–1500 and 600–200 cal yr BP (within dating errors) show a possible correlation to the Holocene ice rafting events in the North Atlantic (i.e., Bond events 1 and 0, Bond et al. 2001). This suggests that late Holocene climatic events in the North Atlantic had counterpart events in the WNLM region.

Forcing mechanism of climatic variability

The increasing trend of $\delta^{13}\text{C}$ values in HN2P-2 implies a trend towards dry and cool conditions, suggesting the influence of decreased solar insolation on an orbital scale (Fig. 5).

Many studies have demonstrated a link between the Asian monsoon intensity and solar activity (Hong et al. 2001; Fleitmann et al. 2003; Weber et al. 2004; Wang et al. 2005; Selvaraj et al. 2012; Zhang et al. 2008; Liu

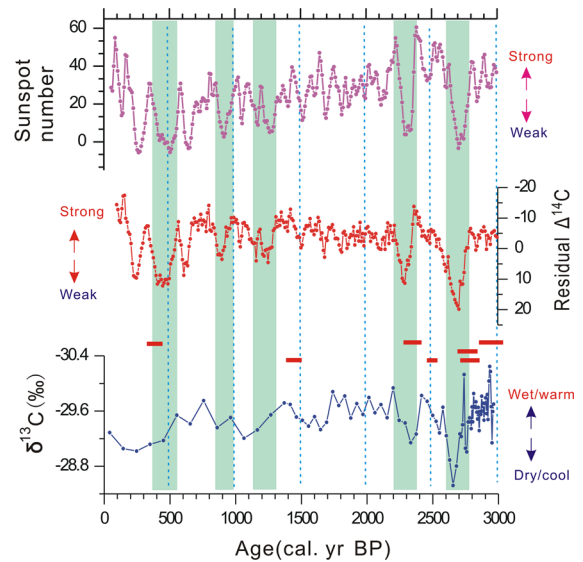


Fig. 5 Correlation of the $\delta^{13}\text{C}$ record of section HN2P-02 in Daping Swamp with the sunspot number record (Solanki et al. 2004) and the residual atmospheric ^{14}C ($\Delta^{14}\text{C}$) record (Stuiver et al. 1998). Seven bulk ^{14}C dates are shown with an uncertainty interval of 2σ . The blue bars indicate some multi-centennial correlations of the three records. (Color figure online)

et al. 2009). Although the resolution of the Daping section is insufficient for direct comparisons on a short time-scale, we find that on a multi-centennial scale, the $\delta^{13}\text{C}$ record generally shows an inverse and a positive correlation with the two proxies of solar activity, i.e., the $\Delta^{14}\text{C}$ (Stuiver et al. 1998) and the sunspot records (Solanki et al. 2004), respectively (Fig. 5). In particular, the correlations are significant for the interval between 2960 and 2200 cal. yr BP. Using the Redfit program (Schulz and Mudelsee 2002), spectral analysis of the $\delta^{13}\text{C}$ record reveals three statistically significant centennial cycles centered on 396, 110, and 102-yr (above 90 % confidence, Fig. 6). The 396-yr cycle is very similar to the 400 yr cycle indicated by the $\Delta^{14}\text{C}$ record (Sonnett and Suess 1984). The 110-yr cycle is very close to the 113-yr cycle obtained from analysis of the total solar irradiance derived from sunspot activity (Lean et al. 1995; Agnihotri et al. 2002). The 102-yr cycle is very similar to the 104-yr cycle, which is widely present in Asian monsoon records and is considered of solar origin (Neff et al. 2001; Agnihotri et al. 2002; Fleitmann et al. 2003).

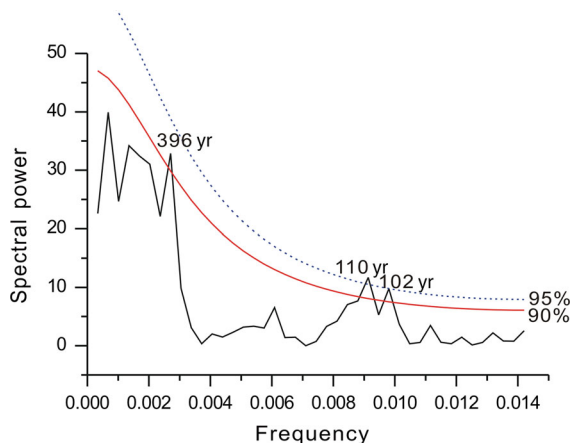


Fig. 6 Estimated periodicities of climatic changes by Redfit analysis derived from the $\delta^{13}\text{C}$ record of HNBP-02 section in Daping Swamp

Conclusions

The evidence gathered for the study region shows a trend towards dry and cold conditions in the late Holocene. We believe that this is because of a decrease in solar insolation on an orbital scale. Three intensified ASM periods, represented by wet and warm conditions, were revealed at ~ 2900 – 2700 , 2500 – 1700 , and ~ 1000 – 600 cal. yr BP. Three weakened ASM periods, which were characterized by dry and cool conditions, were recorded at ~ 2700 – 2500 , 1700 – 1000 and ~ 600 – 200 cal. yr BP. The climatic variability of this study is generally identical to various other Chinese monsoon records, reflecting similar multi-centennial monsoonal variation. This study demonstrates that solar irradiance may have played a role in the variation of ASM intensity. Increased solar irradiance favors strengthened ASM intensity, whereas decreased solar irradiance would result in weakened ASM intensity. Although the peat section is not suitable for high-resolution paleoclimatic study and it has not been possible to discern the individual influence of the two summer monsoon systems (i.e., the EAM and IM), this study presents a unique climatic history of the late Holocene in the WNLM region. Our findings show that in the future more precise dating of the sedimentary sequence in the Daping Swamp could improve our understanding of the variation of the Asian monsoon and its effect on global climatic change over geological time scales.

Acknowledgments Radiocarbon dates were measured in the Key Lab. of Western China's Environmental Systems (Ministry of Education of China), Lanzhou University. Organic carbon isotopes were analyzed in State Key Lab. of Gas Geochemistry, Lanzhou Institute of Geology, CAS. We feel grateful to Mr. Cao Jixiu and Prof. Zhang Chengjun in Lanzhou University and Dr. Yang Hui in Lanzhou Institute of Geology (CAS) for their help in laboratory analyses. We sincerely thank Prof. Steffen Mischke (the Associate Editor of this Journal) and two anonymous reviewers, for their thorough comments and constructive suggestions which significantly improved the manuscript. This work was supported by the Natural Science Foundation of China (Nos. 41071137 and 40671189), the Research Program of Institution of High Education in Guangdong Province for High-level Talents, and the Natural Science Foundation of Guangdong Province (Nos. S2011010003413 and 8151063101000044).

References

- Aaby B (1976) Cyclic climatic variations in climate over the last 5500 years reflected in raised bog. *Nature* 263:281–284
- Agnihotri R, Dutta K, Bhushan R, Somayajulu BLK (2002) Evidence for solar forcing on the Indian monsoon during the last millennium. *Earth Planet Sci Lett* 198:521–527
- An ZS, Kutzbach JE, Prell WL, Porter SC (2001) Evolution of Asian monsoon s and phased uplift of the Himalaya-Tibetan plateau since Late Miocene times. *Nature* 411:62–66
- Berger A, Loutre MF (1991) Insolation values for the climate of the last 10 million years. *Quat Sci Rev* 10:297–317
- Blaauw M (2010) Out of tune: the dangers of aligning proxy archives. *Quat Sci Rev* 36:38–49
- Bond G, Kromer B, Beer J, Muscheler R, Evans M, Showers W, Hoffmann S, Lotti-Bond R, Hajdas I, Bonani G (2001) Persistent solar influence on North Atlantic climate during the Holocene. *Science* 294:2130–2136
- Cai YJ, Tan LC, Cheng H, An ZS, Edwards RL, Kelly MJ, Kong XG, Wang XF (2010) The variation of summer monsoon precipitation in central China since the last deglaciation. *Earth Planet Sci Lett* 291:21–31
- Chai X (1990) Peatland. Geological Publishing House, Beijing, pp 139–140
- Chambers FM, Barber KE, Maddy D, Brew J (1997) A 5500-year proxy-climate and vegetation record from blanket mire at Talla Moss, Borders, Scotland. *Holocene* 7:391–399
- Charman DJ, Caseldine C, Barker A, Gearey B, Hatton J, Proctor C (2001) Paleohydrological records from peat profiles and speleothems in Sutherland, North-west Scotland. *Quat Res* 55:223–234
- Chen FH, Rao ZG, Zhang JW, Jin M, Ma JY (2006) Variations of organic carbon isotopic composition and its environmental significance during the last glacial on western Chinese Loess Plateau. *Chin Sci Bull* 51:1593–1602
- Christopher JE, John H (2000) Climatic control of blanket mire development at Kentra Moss, North-west Scotland. *J Ecol* 88:869–889

- Desprat S, Sánchez-Goni MF, Loutre MF (2003) Revealing climatic variability of the last three millennia in north-western Iberia using pollen influx data. *Earth Planet Sci Lett* 213:63–78
- Dykoski CA, Edwards RL, Cheng H, Yuan DX, Cai YJ, Lin YS (2005) A high-resolution, absolute-dated Holocene and deglacial Asian monsoon record from Dongge Cave, China. *Earth Planet Sci Lett* 233:71–86
- Farquhar GD, Ehleringer JR, Hubick KT (1989) Carbon isotope discrimination and photosynthesis. *Annu Rev Plant Biol* 40:503–537
- Feng X, Epstein S (1995) Carbon isotopes of trees from arid environments and implications for reconstructing atmospheric CO₂ concentration. *Geochim Cosmochim Acta* 59:2599–2608
- Fleitmann D, Burns SJ, Mudelsee M, Neff U, Kramers J, Mangini A, Matter A (2003) Holocene forcing of the Indian Monsoon recorded in a stalagmite from Southern Oman. *Science* 300:1737–1739
- Gao YX, Xu SY, Guo QY (1962) Monsoon region and regional climate in China. In: Gao YX, Xu SY (eds) *Some problems of East Asian Monsoon*. Science Press, Beijing, pp 49–63 (in Chinese)
- Hatté C, Antoine P, Fontugne M, Lang A, Rousseau D, Zöller L (2001) $\delta^{13}\text{C}$ of loess organic matter as a potential proxy for paleoprecipitation. *Quat Res* 55:33–38
- Hong YT, Wang ZG, Jiang HB, Lin QH, Hong B, Zhu YX (2001) A 6000-year record of changes in drought and precipitation in northeastern China based on a $\delta^{13}\text{C}$ time series from peat cellulose. *Earth Planet Sci Lett* 185:111–119
- Hong YT, Hong B, Lin QH, Shibata Y, Hirota M, Zhu YX, Leng XT, Wang Y, Wang H, Yi L (2005) Inverse phase oscillations between the East Asian and Indian Ocean summer monsoons during the last 12000 years and paleo-El Niño. *Earth Planet Sci Lett* 231:337–346
- Hong B, Hong YT, Lin QH, Shibata Y, Uchida M, Zhu YX, Leng XT, Wang Y, Cai CC (2010) Anti-phase oscillation of Asian monsoons during the Younger Dryas period: evidence from peat cellulose $\delta^{13}\text{C}$ of Hani, Northeast China. *Palaeogeogr Palaeoclimatol Palaeoecol* 297:214–222
- Janssens JA (1983) A quantitative method for stratigraphic analysis of bryophytes in Holocene peat. *J Ecol* 171:189–196
- Kohn MJ (2010) Carbon isotope composition of terrestrial C3 plants as indicator of (paleo)ecology and (paleo)climate. *PNAS* 107:19691–19695
- Lean J, Beer J, Bradley R (1995) Reconstruction of solar irradiance since 1610: implications for climate change. *Geophys Res Lett* 22:3195–3198
- Liu ZH, Henderson ACG, Huang YS (2006) Alkenone-based reconstruction of late-Holocene surface temperature and salinity changes in Lake Qinghai. *China Geophys Res Lett* 33:L09707. doi:10.1029/2006GL026151
- Liu XQ, Dong HL, Yang XD, Herzsuh U, Zhang EL, Stuet JBW, Wang YB (2009) Late Holocene forcing of the Asian winter and summer monsoon as evidenced by proxy records from the northern Qinghai-Tibetan Plateau. *Earth Planet Sci Lett* 280:276–284
- Ljungqvist FC (2010) A new reconstruction of temperature variability in the extra-tropical northern Hemisphere during the last two millennia. *Geografiska Ann: Ser A Phys Geogr* 92:339–351
- Neff U, Burns SJ, Mangini A, Mudelsee M, Fleitmann D, Matter A (2001) Strong coherence between solar variability and the monsoon in Oman between 9 and 6 kyr ago. *Nature* 411:290–293
- Qian W, Lin X, Zhu Y, Xu Y, Fu J (2007) Climatic regime shift and decadal anomalous events in China. *Clim Chang* 84:167–189
- Reimer PJ, Baillie MGL, Bard E, Bayliss A, Beck JW, Blackwell PG, Ramsey CB, Buck CE, Burr GS, Edwards RL, Friedrich M, Grootes PM, Guilderson TP, Hajdas I, Heaton TJ, Hogg AG, Hughen KA, Kaiser KF, Kromer B, McCormac FG, Manning SW, Reimer RW, Richards DA, Southon JR, Talamo S, Turney CSM, van der Plicht J, Weyhenmeyer CE (2009) IntCal09 and Marine09 radiocarbon age calibration curves, 0–50,000 years cal BP. *Radiocarbon* 51:1111–1150
- Schulz M, Mudelsee M (2002) REDFIT: estimating red-noise spectra directly from unevenly spaced paleoclimatic time series. *Comput Geosci* 28:421–426
- Selvaraj K, Wei KY, Liu KK, Kao SJ (2012) Late Holocene monsoon climate of northeastern Taiwan inferred from elemental (C, N) and isotopic ($\delta^{13}\text{C}$, $\delta^{15}\text{N}$) data in lake sediments. *Quat Sci Rev* 37:48–60
- Solanki SK, Usoskin IG, Kromer B, Schussler M, Beer J (2004) An unusually active Sun during recent decades compared to the previous 11,000 years. *Nature* 431:1084–1087
- Sonnert CP, Suess HE (1984) Correlation of bristlecone pine ring width with atmospheric ^{14}C variations: a climate-sun relation. *Nature* 307:141–143
- Stebich M, Mingram J, Moschen R, Thiele A, Schröder C (2011) Comments on Anti-phase oscillation of Asian monsoons during the Younger Dryas period: evidence from peat cellulose delta 13C of Hani, Northeast China by B. Hong et al. [*Palaeogeogr, Palaeoclimatol, Palaeoecol* 297(2010) 214–222]. *Palaeogeog Palaeoclimatol Palaeoecol* 310:464–470
- Stuiver M, Reimer PJ, Braziunas TF (1998) High-precision radiocarbon age calibration for terrestrial and marine samples. *Radiocarbon* 40:1127–1151
- Sun SY, Zhang JE (1984) Pollen combination of the Daping peat deposit in Hunan and its formation environment. *J Nanjing Nor Uni* 4:86–92 (in Chinese)
- Wang GA, Han JM, Zhou LP (2002) The annual average temperature in northern China. *Chin J Geol* 29:55–57 (in Chinese)
- Wang GA, Han JM, Liu TS (2003) The carbon isotope composition of C3 herbaceous plants in loess area of northern China. *Sci China (Ser D: Earth Sci)* 46:1067–1076
- Wang YJ, Cheng H, Edwards RL, He Y, Kong X, An ZS, Wu J, Kelly MJ, Dykoski CA, Li X (2005) The Holocene Asian Monsoon: links to solar changes and North Atlantic climate. *Science* 308:854–857
- Wang H, Hong YT, Lin QH, Hong B, Zhu YX, Wang Y, Xu H (2010) Response of humification degree to monsoon climate during the Holocene from the Hongyuan peat bog, eastern Tibetan Plateau. *Palaeogeogr Palaeoclimatol Palaeoecol* 286:171–177
- Weber SL, Crowley TJ, van der Schrier G (2004) Solar irradiance forcing of centennial climate variability during the Holocene. *Clim Dynam* 22:539–553

- White JWC, Ciais P, Figge RA, Kenny R, Markgraf V (1994) A high-resolution record of atmospheric CO₂ content from carbon isotopes in peat. *Nature* 367:153–156
- Xiao YT, Cao TR, Pen ZH (1986) Mapping the vegetation (1:50000) of the Nanshan Mountain of Chengbu county, Hunan Province. *J Cent South Forest Coll* 6:34–40 (in Chinese)
- Yancheva G, Nowaczyk NR, Mingram J, Dulski P, Schettler G, Negendank JFW, Liu JQ, Sigman DM, Peterson LC, Haug GH (2007) Influence of the intertropical convergence zone on the East Asian monsoon. *Nature* 445:74–77
- Yang B, Bräuning A, Dong ZB, Zhang ZY, Jiao KQ (2008) Late Holocene monsoonal temperate glacier fluctuations on the Tibetan Plateau. *Global Planet Chang* 60:126–140
- Zhang PZ, Cheng H, Edwards RL, Chen FH, Wang YJ, Yang XL, Liu J, Tan M, Wang XF, Liu JH, An CL, Dai ZB, Zhou J, Zhang DZ, Jia JH, Jin LY, Johnson KR (2008) A test of climate, sun, and culture relationships from an 1810-Year Chinese cave record. *Science* 322:940–942
- Zhang JW, Chen FH, Holmes JA, Li H, Guo XY, Wang JL, Li S, Lü YB, Zha Y, Qiang MR (2011) Holocene monsoon climate documented by oxygen and carbon isotopes from lake sediments and peat bogs in China: a review and synthesis. *Quat Sci Rev* 30:1973–1987
- Zhong W, Ma QH, Xue JB, Zheng YM, Cai Y, Ouyang J (2010) Humification degrees of a lacustrine sedimentary sequence as an indicator of past climatic changes in the last c 49000 years in South China. *Boreas* 39:286–295
- Zhou WJ, Yu XF, Timothy JAJ, Burr G, Xiao JY, Lu XF, Xian F (2004) High-resolution evidence from southern China of an early Holocene optimum and a mid-Holocene dry event during the past 18000 years. *Quat Res* 62:39–48